Ref. Ares(2024)5765500 - 09/08/2024

ROADVIEW

Robust Automated Driving in Extreme Weather

Project No. 101069576

Deliverable 5.5

Environmental and weather condition state estimates

WP 5 – Robust perception system

Authors	Matti Kutila (VTT), Topi Miekkala (VTT), Mikko Tarkiainen (VTT), Jyri Maanpää (FGI), Isabelle Morvan (CRF)
Lead participant	VTT
Delivery date	09 August 2024
Dissemination level	Public
Type	Document, report

Version 1.0

Funded by the European Union

Innovate UK

Funded by the European Union (grant no. 101069576). Views and opinions expressed are however those of the author(s) only and do not necessarily reflect those of the European Union or European Climate, Infrastructure and Environment Executive Agency (CINEA). Neither the European Union nor the granting authority can be held responsible for them. UK and Swiss participants in this project are supported by Innovate UK (contract no. 10045139) and the Swiss State Secretariat for Education, Research and Innovation (contract no. 22.00123) respectively.

Revision history

Author(s)	Description	Date
Matti Kutila (VTT)	Draft deliverable	27/03/2024
Matti Kutila (VTT)	Writing the introduction chapter	15/05/2024
Isabelle Morvan (CRF)	Writing the chapter on V2X messaging	22/05/2024
Jyri Maanpää (FGI)	Draft of sections 3 and 4	18/06/2024
Topi Miekkala (VTT)	Visibility estimator added	27/06/2024
Matti Kutila (VTT)	Revision	27/06/2024
Matti Kutila (VTT)	Finalising the content	03/07/2024
Jyri Maanpää (FGI), Matti Kutila (VTT)	Improvements to the chapter 3.1 Grip prediction	16/07/2024
Maikol Funk Drechsler (THI)	Internal Review	31/07/2024
Tuomas Herranen (LUA)	Internal Review	02/08/2024
Matti Kutila (VTT)	Review comment revision	08/08/2024
Matti Kutila (VTT)	Final version	09/08/2024

s

Contents

List of Figures

List of Tables

Partner short names

FGI	Maanmittauslaitos – Finnish Geospatial Research Institute
CRF	Canon Research Centre France
THI	Technische Hochschule Ingolstadt
VTT	Teknologian Tutkimuskeskus VTT OY

Abbreviations

ACDC	Adverse Conditions Dataset with Correspondences dataset
API	Application Programming Interface
CAV	Connected Automated Vehicles
C-ITS	Cooperative Intelligent Transport Systems
D	Deliverable
EC	European Commission
EU	European Union
HEU	Horizon Europe
FPN	Feature Pyramid Network
I2V	Infrastructure to Vehicle
M	Month
MQTT	Message Queue Telemetry Transport
MS	Milestone
ROS	Robot Operating System
RSU	Roadside Unit
RWM	Road Weather Message
SAE	Society of Automotive Engineers
SW	Software
WP	Work Package
V2X	Vehicle-to-Everything

Executive summary

This deliverable provides the results related to the development of the environment and weather condition estimator in the ROADVIEW project, which is conducted under the Horizon Europe Framework Programme within the call HORIZON-CL5-2021-D6-01-01 “More powerful and reliable on-board perception and decision-making technologies addressing complex environmental conditions (CCAM Partnership).” The ROADVIEW project aims to address the challenges posed by adverse weather conditions in the context of highly automated driving, with a particular emphasis on enhancing the reliability and safety of Connected and Automated Vehicles (CAVs).

The weather state estimator is a crucial component within the project scope, designed to enable automation systems to operate effectively in harsh weather conditions. By providing real-time knowledge of the prevailing weather conditions, the estimator supports the decision-making system of CAVs, ensuring that these systems can adapt to variations in sensing distances, trajectory planning, and safety margins. Accurate and timely weather data is critical for maintaining the operational integrity of automated vehicles, as it directly influences sensor performance and overall situational awareness. The development of the weather state estimator is focused on improving the CAV's ability to perceive and react to existing road and weather conditions. This enhancement is particularly important for the optimization of sensor functionality, which is often compromised in challenging environmental scenarios. By refining the CAV’s situational awareness, the project aims to mitigate risks associated with reduced visibility, unpredictable road surfaces, and other weather-induced factors that could impact vehicle performance and safety.

Objectives

This deliverable explains the algorithm and concepts developed for cooperative environment perception status analysis. The weather state estimator provides information about the drivable area, which can change even for human drivers when there are snowbanks or slippery tracks on the road due to water or ice. Additionally, fog and snow affect the sensing ranges, particularly for high-resolution optical sensing devices, thereby reducing time-to-collision and, consequently, the safe driving speed. The grip estimator provides information related to braking distances.

The project has developed visibility range estimators, grip estimators, and drivable area information based on LiDAR and camera data. Furthermore, a module has been developed to exchange information with roadside units. The benefit of roadside data is that it typically comes from more expensive and high-end products compared to cost-sensitive automotive products. The modules are now ready to take the next steps forward and be integrated into the project’s pilot vehicles.

Methodology and implementation

The road weather understanding modules are based on 1) visibility estimation of individual sensors, 2) analysis of the drivable area, and 3) friction estimation. All of these measurements are taken using optical sensing devices: thermal cameras, LiDARs, and regular cameras. The aim is to measure the actual sensing range and available friction to calculate vehicle control parameters, thereby preventing slipping on the road. Moreover, the calculated parameters are not only used internally within the vehicle's control unit but are also shared with other vehicles through the V2X (Vehicle-to-Everything) communication channel. This communication enhances the situational awareness of connected and autonomous vehicles (CAVs) in the vicinity, allowing them to make informed decisions based on the collective data from multiple sources.

Visibility estimation is challenging task since there is not precise standard or understanding what it means. Usually, visibility is compared to the visual range of human eyes. For optical sensors, this is good assumption since most of them are operating in 380 – 750 nm which is also range of the camera vision system when using gray scale or RGB cameras. However, the cameras and LiDARs also cover near-infrared field up to 980 nm but the sensitive does not deviate much from visual bandwidths. In this project, the crucial decision was made to use 24 GHz radar as a reference. This more challenging since millimetre waves penetrate better thought to fog than microwaves. Thus, the visibility estimator calculates visual range of the optical sensing devices compared to radar what automotive industry is using today for emergency braking applications.

The friction prediction system uses RGB camera images and pixelwise lidar reflectance measurements as input modalities, as they provide good results and are easy to fuse together. The model is based on a Feature Pyramid Network (FPN), with separate ResNet34 encoders processing the RGB and reflectance inputs, whose features are then concatenated before the decoder. The model is trained using ground truth grip values and surface layer thicknesses of water, ice, and snow, provided by a mobile road weather sensor.

Another key function, drivable area detection, is based on a convolutional neural network (CNN) trained to perform road area segmentation using an onboard front-facing RGB camera unit. This advanced neural network model processes real-time images captured by the camera, identifying drivable areas from non-drivable areas.

To extend the situational awareness of vehicles, V2X communication units are implemented for a Road Weather C-ITS service station. The aim is to explore the V2X message exchange and the structure of the Road Weather Message, highlighting the benefits of V2X message exchange for weather information sharing.

Outcomes

The main outcomes of this deliverable are the software algorithms that provide the following outputs:

- **Range Estimation**: This determines how far the optical sensing components can see, offering crucial data on the visual range and detection capabilities of the sensors.
- **Drivable Area Estimation**: This estimates which areas in front of the vehicle are drivable, enhancing the vehicle's ability to navigate safely by identifying viable paths and avoiding obstacles.
- **Road Friction Estimation**: This predicts the friction of the road ahead, providing vital information for adjusting driving dynamics, improving safety, and enhancing the performance of braking and traction control systems.
- **V2X Cooperative System**: This feature facilitates the sharing of information between vehicles, enabling a cooperative network where vehicles can communicate and share real-time data about their surroundings, thus improving overall traffic safety and efficiency.

Next steps

The main advancements include the implementation of these components in vehicles as part of Work Package 7 and 8. Initially, the V2X system will undergo field studies using a mobile RSU (Roadside Unit) and subsequently be tested at the Lapland test site in Northern Europe. The visibility estimator, along with the drivable area and friction estimation systems, forms the automated vehicle weather understanding unit. This unit will be integrated into the project's pilot vehicles to adapt the control algorithms accordingly.

1 Introduction

Current automotive automation systems available in the market correspond to SAE Levels 2-3, where the primary responsibility remains with the vehicle driver even though that in level 3 the driver does not have to supervise the car continuously but still human decisions override automation functions. Level 4 automation is expected to be introduced within the next five years, even though highly automated robotaxis are already operating in San Francisco, Phoenix, and Beijing. However, these robotaxis are mainly restricted to operating only in the absence of fog or adverse weather conditions. This project aims to push beyond these limitations, enabling better control functions for vehicles that adapt to actual weather conditions. This progress will pave the way towards Level 5 automation, where automation operates in all conditions and environments. Although fully autonomous vehicles may not become a reality anytime soon, achieving Level 5 automation is anticipated by 2035 but most likely not in original format which means that automation is available without any Operation Design Domain (ODD) restrictions.

This deliverable is related to the work carried out in the ROADVIEW project, Task 5.3 (Environmental and Weather Condition State Estimation). The work has been divided into three parts according to the partners' fields of expertise and responsibilities in the project:

- VTT: Visibility state estimator
- CRF: V2X support for weather measurements
- FGI: Slipperiness monitoring
- FGI: Drivable area detection

The aim of this work is to improve CAV situation awareness of existing road and weather conditions, with a particular focus on influencing sensor performance. Sensor range vs. resolution has been the primary challenge in enabling high-speed automated driving. One example is using high-definition mapping [1] for this purpose, but a drawback is the need to constantly update the map database. Therefore, this project aims to understand reliable visibility ranges for on-board object recognition and to control the vehicle according to the available sensing performance. This represents a significant improvement for driving at low speed, avoiding the need to come to a full stop when visibility is limited.

The aim is to ultimately integrate the components into the vehicles' weather conditional decision maker [7]. This integration is carried out in the project's WP7 X-in-the-loop test environment and WP8 Integration and Demonstration phase, where different vehicles adopt the necessary modules in a tailored manner. Each vehicle will be equipped with modules specifically designed to enhance its performance under varying weather conditions. The integration process involves rigorous testing and validation to ensure that each module functions correctly and interacts seamlessly with the vehicle's existing systems. The modules play a crucial role in adapting vehicle controls, such as speed, acceleration, and safety margins, based on real-time weather data. This adaptive control is essential for maintaining optimal performance and safety in diverse weather conditions.

In addition to basic control adjustments, the modules are designed to support planning for minimum risk manoeuvring (MRM). This involves calculating the safest possible manoeuvres the vehicle can execute in response to sudden changes in weather conditions or unexpected obstacles. By incorporating MRM capabilities, the vehicle can make intelligent decisions that prioritize passenger safety and minimize the risk of accidents.

2 On-board visibility estimator

2.1 Visibility estimator principle

Estimating the absolute visibility of perception sensors in an automated vehicle presents a challenge due to several factors. Many vehicles implement perception algorithms that fuse multi-modal sensor data to make final decisions about their surroundings. For example, vehicle systems might use data from a 2D RGB camera, a 3D point cloud obtained from a lidar, and a 2D point cloud from an automotive radar. Each of these sensors behaves very differently in adverse weather conditions. In heavy snowfall, an RGB camera's view often turns 'foggy,' reducing image sharpness and detail for distant targets, while individual snow particles might not be clearly visible due to camera exposure time. Conversely, a lidar's 3D point cloud can register significant particle noise, and snow particles in front of the vehicle might be interpreted as major obstacles by the vehicle algorithms (see Figure 1). Meanwhile, an automotive radar can see through snow, fog, and rain particles with much greater robustness, although it provides somewhat limited information compared to the camera and lidar. Various other sensor types with different properties are often included in vehicle sensing systems.

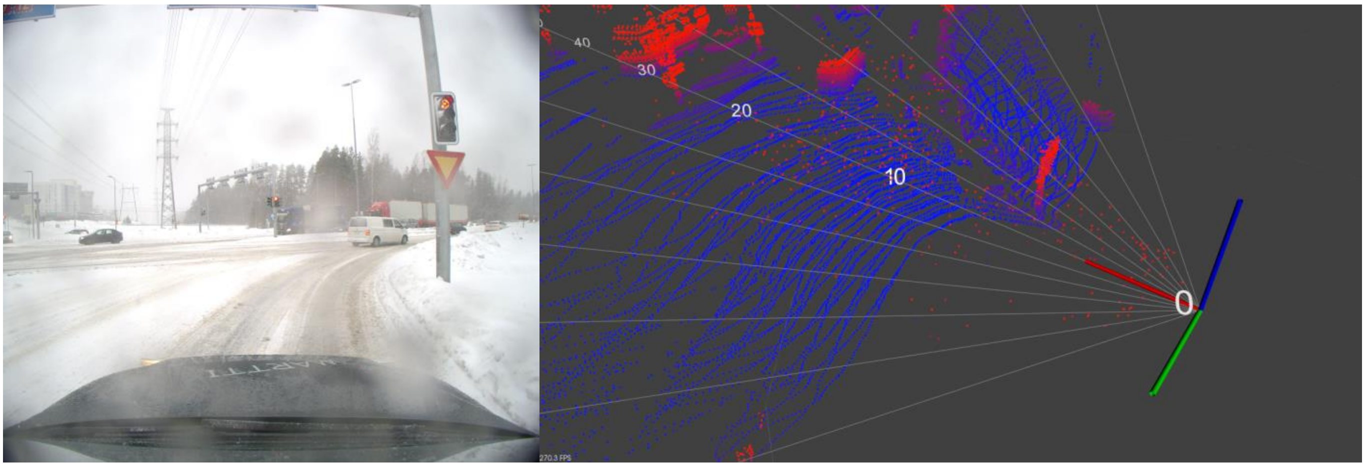

Figure 1. Effect of snowfall on camera image and lidar point cloud.

This creates a problem when defining visibility for the perception system (Figure 2). Since the same weather condition affects each individual sensor differently, deciding on a single metric to represent the visibility of the entire vehicle can be challenging. Another important factor in estimating visibility at each timestep is the traffic scenario the vehicle is currently in. For example, a vehicle might be driving in perfectly clear weather on a highway with another vehicle in front blocking its sensors' view. This results in a situation where the trailing vehicle might have visibility of just a few tens of meters directly in front, but more than 100 meters in other directions. This type of occlusion could be addressed by splitting the observed areas into smaller sectors and estimating the visibility for each sector to obtain more accurate information.

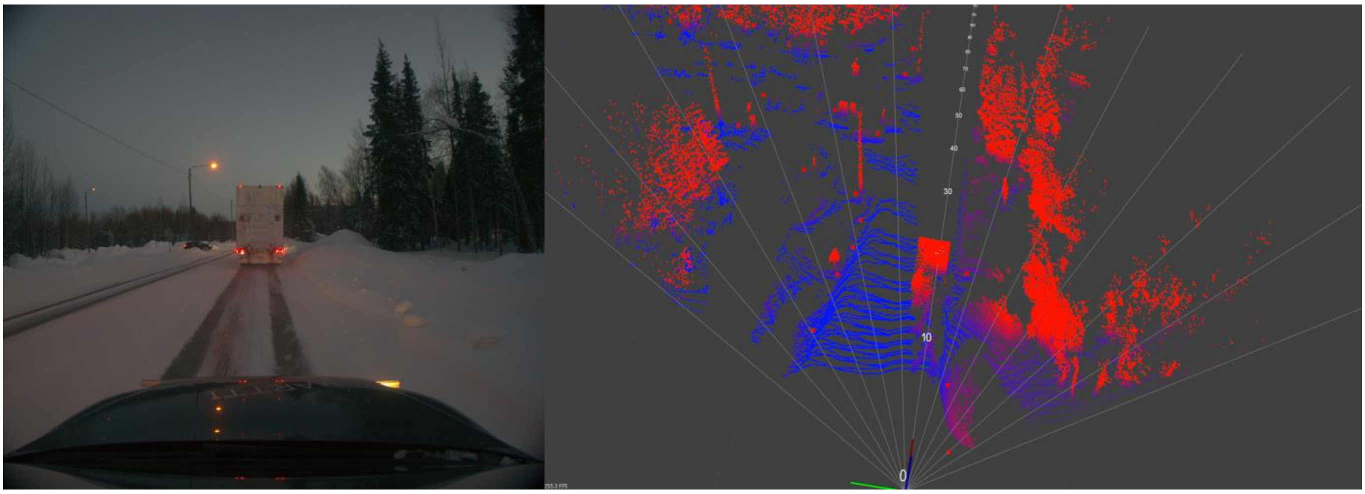

Figure 2. Partial occlusion unrelated to adverse conditions.

2.2 Sensor hardware

The VTT self-driving research vehicle Martti was used to collect the preliminary data to develop visibility estimation. The most relevant sensors included a Basler A2A2600-20GCBAS RGB camera, an e-con systems CU20 HDR camera, a Livox HAP 905 nm lidar, a Luminar H3 1550 nm lidar, an Ouster OS1-64 865 nm lidar, and a Continental ARS-408 automotive radar. Additionally, positioning-related data was collected using a Ublox ZED-F9P GNSS sensor, an Xsens MTi-680g inertial sensor, and the vehicle's CAN bus for various odometry data. The data was collected for offline development, with the GNSS, IMU, and vehicle odometry data used to synchronize the measurements of the different perception sensors. Three lidar sensors with different properties were recorded, as the goal was to estimate the 3D visibility state using the lidar point clouds.

2.3 Estimation method

The initial development focuses on estimating the visibility of the lidar sensor, whose view distance is often most impaired in adverse weather. The variance between different lidar resolutions and scan patterns should also be considered. When determining how to estimate visibility, specific criteria and thresholds must be established. For example, what is the minimum number of points, or their density, that must be met to consider an area visible or not visible? If a single solitary 3D point is reflected without any nearby neighbours, it cannot be make any assumptions about the target it is reflected from. However, if a few 3D points in close proximity to each other are reflected, it can be be much more confident that a target actually exists at those coordinates. Deciding what is considered 'close proximity' should depend on the lidar's resolution and view distance. A visual example using the Ouster OS1-64 lidar is shown in Figure 3.

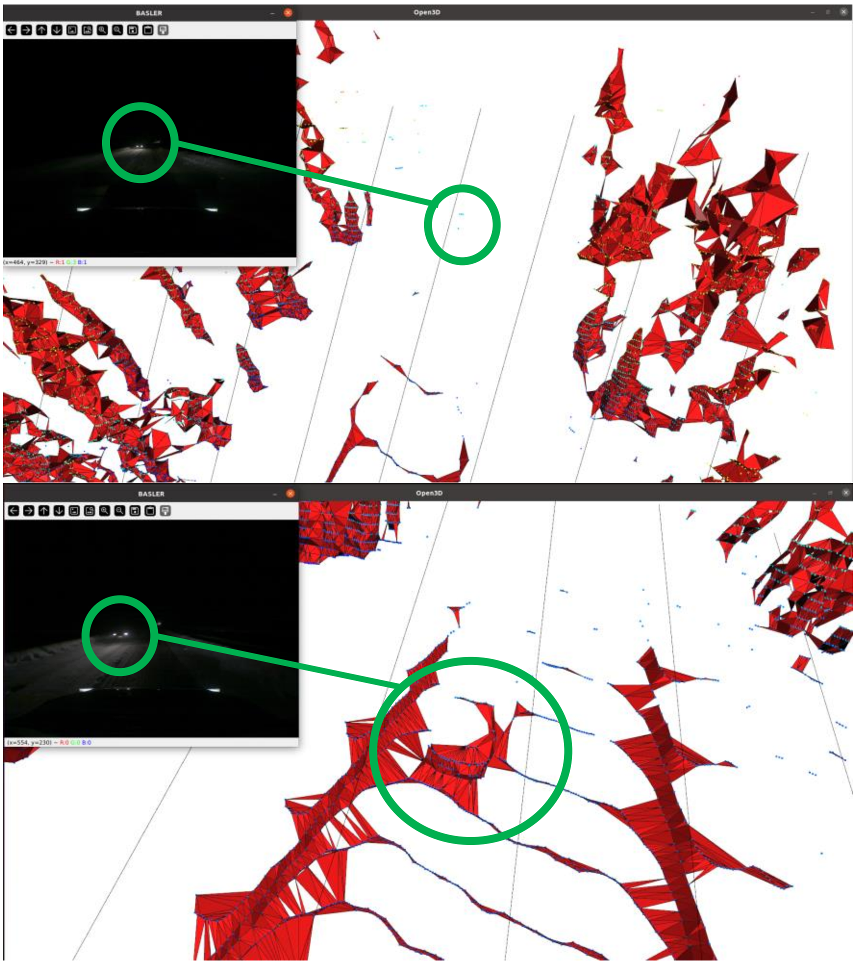

Figure 3. Far away object reflecting unreliable low amount of points (above image). Closer object reflecting sufficient points for machine vision algorithms (below image).

The estimation of these point cloud structures can be performed using algorithms that find neighbouring points based on distance parameters. These connections are made between all 3D points in the point cloud. The point cloud area is then split into sectors for the reasons described in the introduction. In each sector, the farthest distance with enough 3D points for reliable reflections is identified. This distance is then defined as the visibility in meters for that part of the point cloud.

2.4 Software description

Testing of different approaches has been implemented in Python, specifically using the tools available in the Open3D library, which offers tools for point cloud and mesh processing. The mesh tools, especially, have been utilized in automating the estimation of point connections (see Figure 4). Methods have been tested where the point cloud is processed in distance slices every 10 meters. At each distance slice, a threshold for the point-to-point distance is calculated based on the vertical resolution of the lidar sensor as $\gamma = d\tan(\alpha)$ where d is the point-to-point distance threshold and α is the lidar vertical resolution. A mesh surface is then reconstructed automatically using the Open3D library's alpha shapes method. The alpha shapes method of mesh creation can be briefly described as repeatedly attempting to insert a circle of radius γ into the point cloud. If the circle fits without colliding with points, the area is considered not part of the mesh. Conversely, if the inserted circle collides with points, they are considered close enough to each other to form a mesh surface [21].

After processing the distance slices, the resulting mesh is stepped through in angular sectors. For each angular sector, the resulting mesh from the previous step is clustered using Open3D automated functions. The mesh triangles and vertices are clustered based on their connections to each other; if a set of triangles and vertices are connected based on the alpha shape generation, that set is considered a single cluster object. The formed set of clusters at each angular sector is filtered by a surface area threshold requirement to eliminate objects with only one or two vertex points. Then, the furthest object is considered, and the mean 3D coordinates are chosen as the visibility distance for that sector.

The constraints of the mesh creation should be improved. Currently, the distance threshold is selected based on the vertical resolution of the lidar sensor, which is reasonable when detecting targets perpendicular to the sensor but not ideal for detecting surfaces parallel to the lidar view direction, such as the ground plane. Additionally, situations can occur where the point cloud is empty in one direction, not because of adverse weather, but simply because there are no targets. This should be considered in the calculations.

The goal is to test and develop the visibility estimation using the point cloud and mesh library tools for simplicity and exporting potentially applicable versions to a C++ environment to operate in the vehicle in real time. Initial tests making use of a neural kernel field-based 3D reconstruction have also been made to examine if environment reconstruction could be utilized in the development of the algorithms.

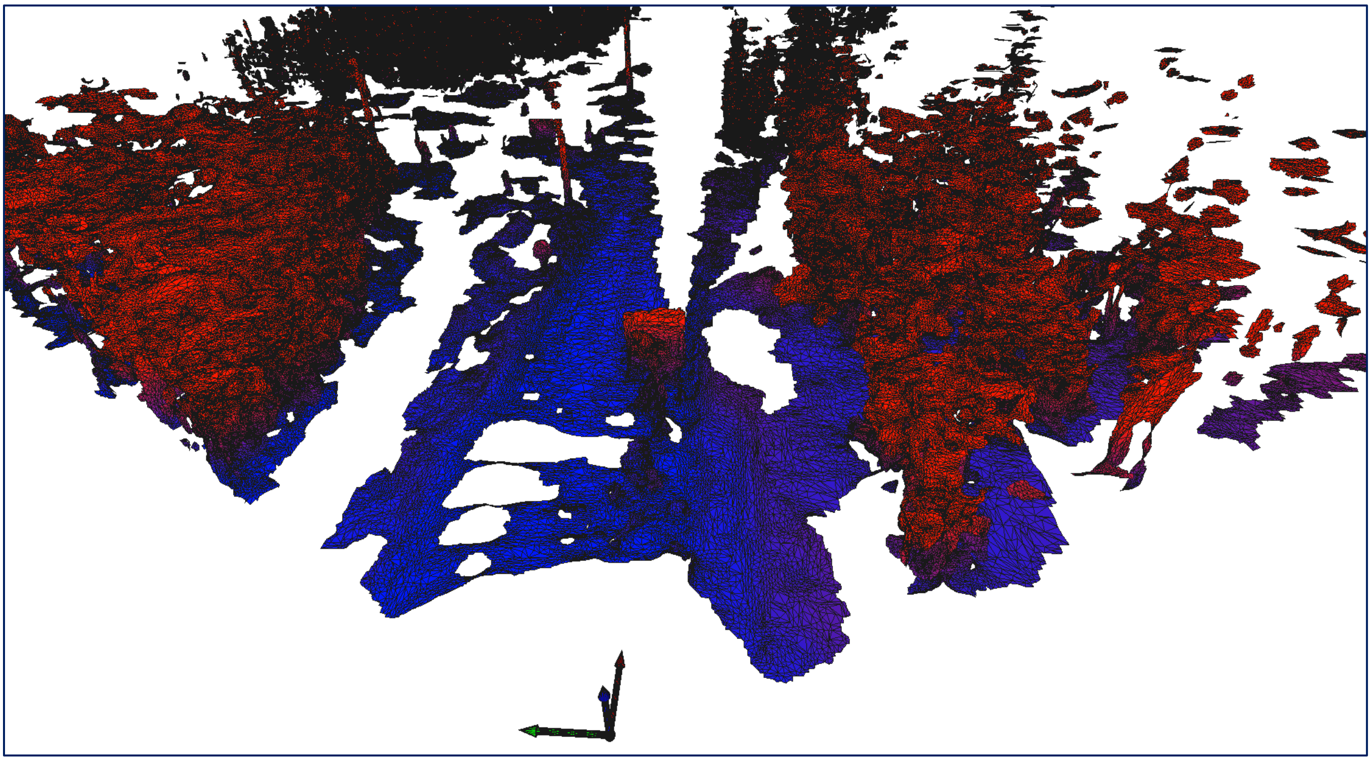

Figure 4. 3D reconstruction of a single Luminar point cloud (same scene as Figure 2) using NKSR framework.

3 Slipperiness monitoring

This section describes the slipperiness monitoring module, which has been more precisely described in [8]. The main outcomes of the article have been summarised in the following sub-chapters.

3.1 Summary of the grip prediction method

The grip measurement methods are based either on contact-based methods [13] or non-contact-based methods [16]. These methods provide single-point measurements for the grip of the road, but they cannot predict the grip ahead of the vehicle. There are computer vision methods which also predict the grip within the road area in front of the car, but they are either limited to a single grip prediction for the complete road area [18] or a coarse grip classification within a pre-defined low-resolution grid in front of the car [19]. Our work extends the previous research by predicting scalar grip values over a dense map on the road area.

In order to have the necessary training data for the task, we collected a dataset of 237,000 (37 hours, 1538km) matched image, lidar, and grip measurement frames with our research platform ARVO (see Figure 5). The ground truth of pixelwise grip measurements is obtained from a mobile road weather sensor (Vaisala MD30), which estimates the grip on a single measurement spot based on infrared spectroscopy. The measured points are then projected onto the camera image with the car's GNSS trajectory information, time synchronization, and 3D-transforms between different sensor frames. Therefore, the image data is matched with pixelwise grip values which are to be measured as the car drives along the trajectory seen in the image.

Figure 5. The instrumented research vehicle ARVO used in the data collection.

Our proposed grip prediction model is shown in Figure 6. The RGB camera and pixelwise lidar reflectance measurements provide relatively good results and they are also easy to fuse together, so they are used as the input modalities for the model. The model is a Feature Pyramid Network (FPN) [15] with the exception that the RGB and reflectance modalities are processed with separate ResNet34 encoders and their features are concatenated before the decoder. The model is trained with ground truth grip values, surface layer thicknesses of water, ice, and snow and the road weather state all of which are also provided by the mobile road weather sensor. In addition, the model predicts the standard deviation estimate of the grip prediction which is trained with a specific loss function from [14]. The surface layer thickness prediction is only used as an auxiliary supportive task for the grip prediction model as the other outputs of the model are used in the following grip uncertainty prediction step.

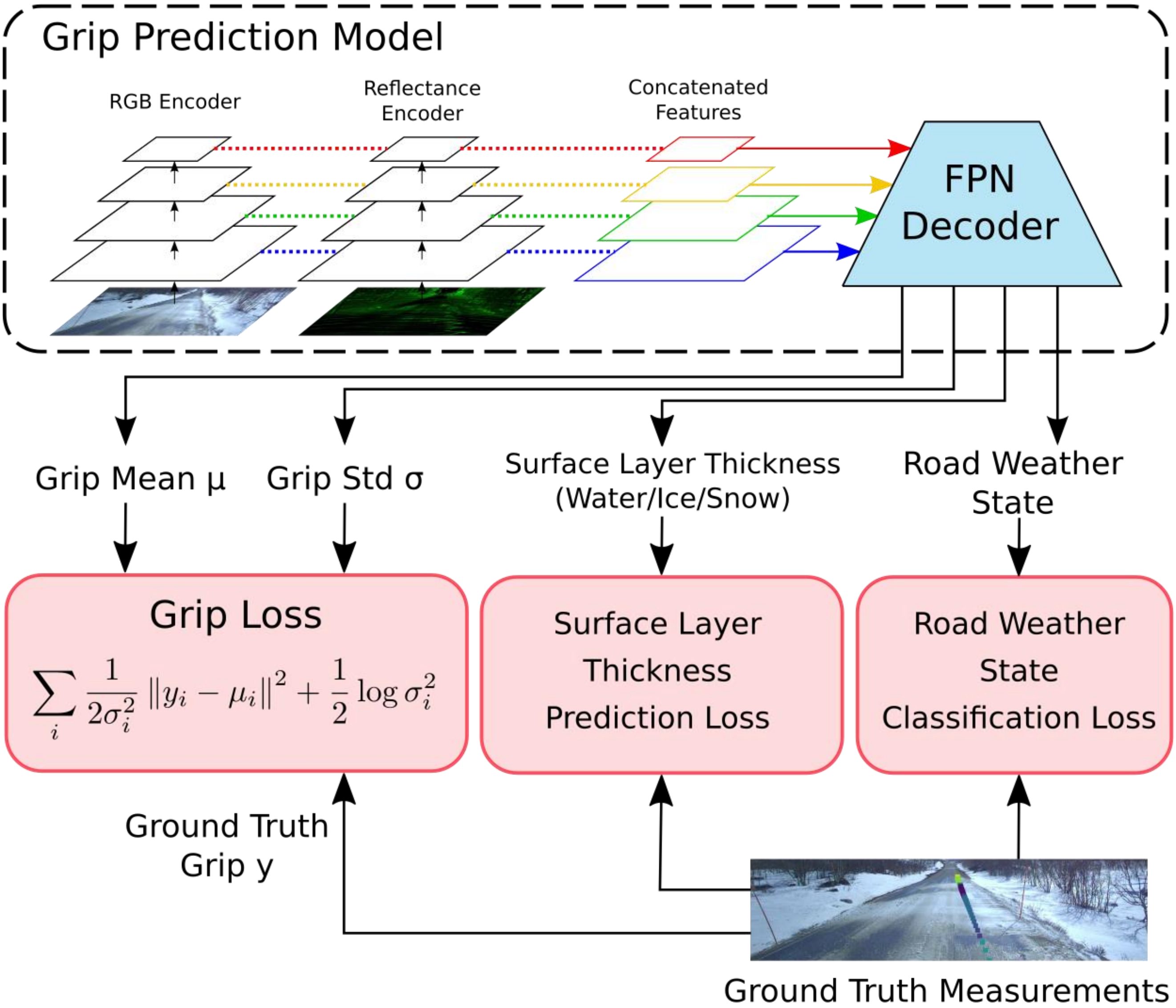

Figure 6. Grip prediction model.

3.2 Grip uncertainty prediction

In addition to the grip prediction, we extended the model presented in [8] to perform grip uncertainty prediction. We fused two different approaches to obtain a pixelwise probability distribution for the grip output values. The first approach is based on the work in [14] with the assumption that the grip probability distribution is Gaussian. Therefore we predicted the mean and standard deviation of the grip output with a special loss function presented in the reference. The second approach is that, in addition to grip mean and standard deviation estimates, we predict the road weather class provided by the road weather sensor (the included classes are dry/moist, wet, snowy, icy, and slushy road conditions). As we have predetermined the grip distribution for different road weather classes which are provided by the road weather sensor, we can fuse the class probabilities to obtain a grip probability distribution based on the road weather class estimates from the model. Finally, we can fuse these two probability distributions to have a single, more accurate probability distribution for each predicted grip value. The grip uncertainty prediction is illustrated in Figure 7.

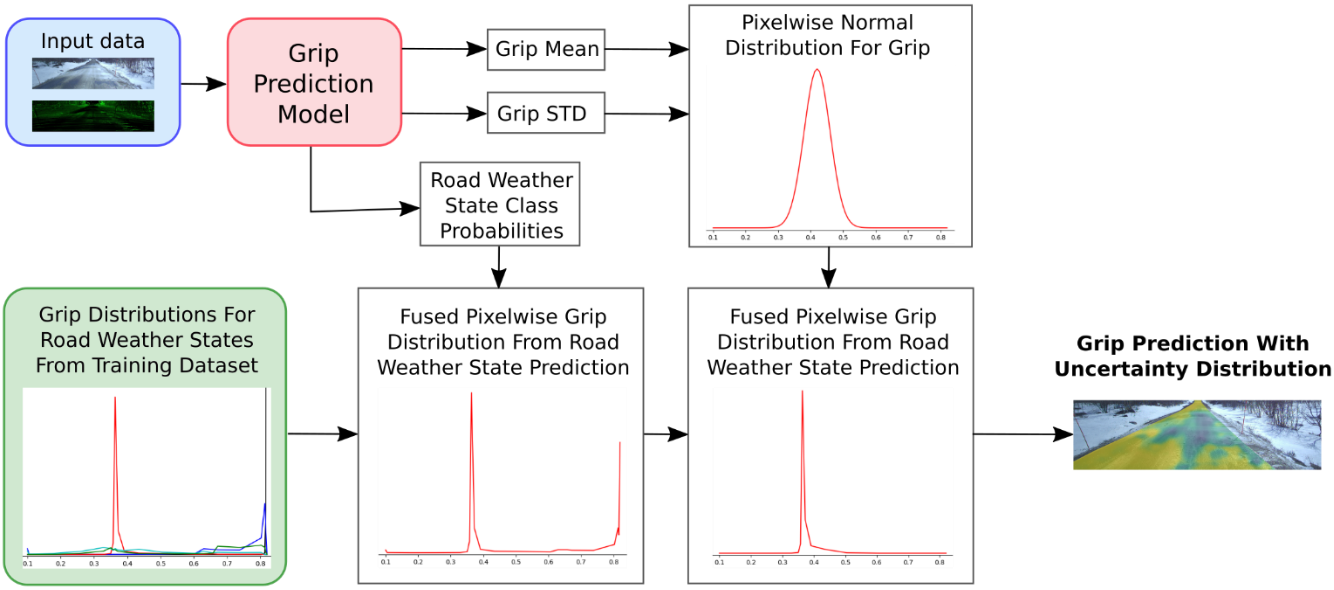

Figure 7. Grip uncertainty prediction.

3.3 Results

The grip and grip uncertainty prediction results of the model in the validation set, test set, and additional extra drives are presented in Table 1. The metrics used are the mean squared error of the mean grip value from the grip probability distribution when compared to the ground truth values, a similar metric with the median grip from the grip distribution, the number of ground truth values within 95% and 68.2% confidence intervals, the average length and the left limit position of the 95% confidence interval, and the accuracy of the road weather state prediction. In the analysis, the right confidence interval limits were increased by a value of 0.01 in order to include the most prominent grip values at the right end of the scale (value 0.82, the grip of dry road) within the confidence interval. We observe that the accuracy of the model (mean grip value from the grip probability distribution) when compared to the ground truth from the road weather sensor data could be slightly less accurate than in the work in Appendix 1, but the difference is really small. The number of ground truth values which are within the 95% confidence interval is 96.4 in the test set, which shows that the uncertainty distribution follows the actual grip uncertainty. The lower limit of the 95% confidence interval is also relatively large (value 0.628), meaning that the grip uncertainty would not be unnecessarily low in most of the cases to maintain correct predictions within confidence intervals. The results in separate test drives have higher variance, as these contain only a small set of road weather conditions.

Table 1. The grip uncertainty prediction model results on the validation set, test set and three separate test drives.

	Validation set	Test set	Test drive 1	Test drive 2	Test drive 3
Mean squared error of predicted grip distribution **mean**	0.0681	0.0620	0.1021	0.1562	0.0805
Mean squared error of predicted distribution **median**	0.0701	0.0642	0.1053	0.1597	0.0819
Amount of predictions **within 95%** confidence intervals **(%)**	95.5	96.4	83.9	79.4	91.4

Amount of predictions **within 68.2% c**onfidence intervals **(%)**	83.4	85.2	61.5	54.5	70.3
Average **length of grip 95% confidence interval**	0.109	0.104	0.185	0.313	0.161
Average **position of the lower 95% confidence interval limit**	0.615	0.628	0.350	0.322	0.647
Road weather state prediction accuracy (%)	94.1	94.8	72.7	41.2	80.9

Figure 8 showcases some example grip predictions along with their uncertainty estimates under various conditions. It is evident from our observations that our method is capable of accurately tracking the grip of the road. Furthermore, it provides a comprehensive understanding of the uncertainty associated with these predictions, thereby enhancing the reliability of the system. However, the grip prediction has challenges in road conditions rarely observed in the training data and in the detection of small local areas with a different grip (such as narrow tire tracks clear of snow). In addition, it’s important to note that this method does not distinguish between the road area and the non-road area. Therefore, additional methods are required for the detection of drivable areas. A method specifically designed for drivable area segmentation is elaborated upon in the subsequent section.

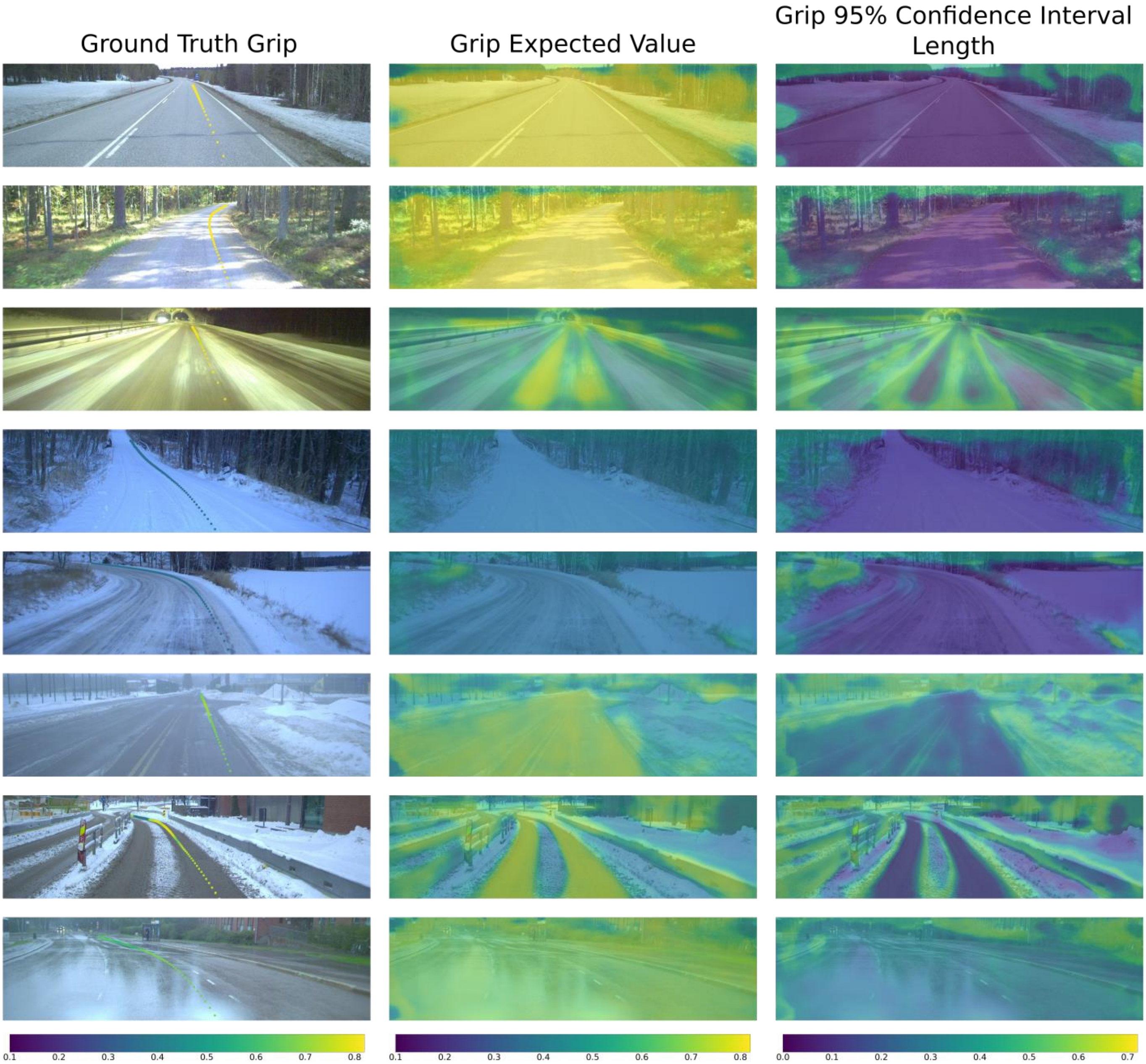

Figure 8. Examples of grip uncertainty prediction.

4 Drivable area detection

There are fewer public autonomous driving datasets available that encompass diverse road weather conditions and semantic segmentation classes for drivable or road areas. The ACDC dataset (Adverse Conditions Dataset with Correspondences) [20] includes 4000 frames with Cityscapes segmentation classes, but it only contains samples from urban areas and lacks examples of heavy snow conditions. The Mapillary Vistas dataset [17] also offers a diverse representation of different road conditions from various continents, but it does not cover a wide range of snowy conditions.

To produce a drivable area segmentation mask to limit grip prediction output, the method from our prior work [9] has been implemented. This work presents a convolutional neural network trained to perform both road area segmentation and car steering wheel angle prediction from front-facing RGB camera images in cars. The road area segmentation is obtained from the Mapillary Vistas dataset, and the steering wheel angles are sourced from a previous dataset from the Finnish Geospatial Research Institute. This steering dataset provides a broad representation of different winter conditions, making it suitable for this task. The convolutional neural network is trained with both datasets in such a way that training on the steering dataset initiates transfer learning to the challenging conditions in that dataset. We used the model based on FPN with a ResNet 18 encoder and all other details on model architecture and training can also be found in the mentioned previous work.

Examples of road area segmentation are shown in Figure 9. It was observed that the road segmentation masks are of medium quality due to the lack of annotated training data in adverse weather conditions. Additionally, the model's performance is impacted by variations in camera orientation and calibration, as it was designed to be supported by the steering task in a specific camera setup. Originally, the road area segmentation accuracy (mean Intersection over Union) is 90.61% on a challenging dataset with 100 samples [8]. However, the quality of the image masks is sufficient to visualize the performance of the grip prediction task discussed in the previous chapter.

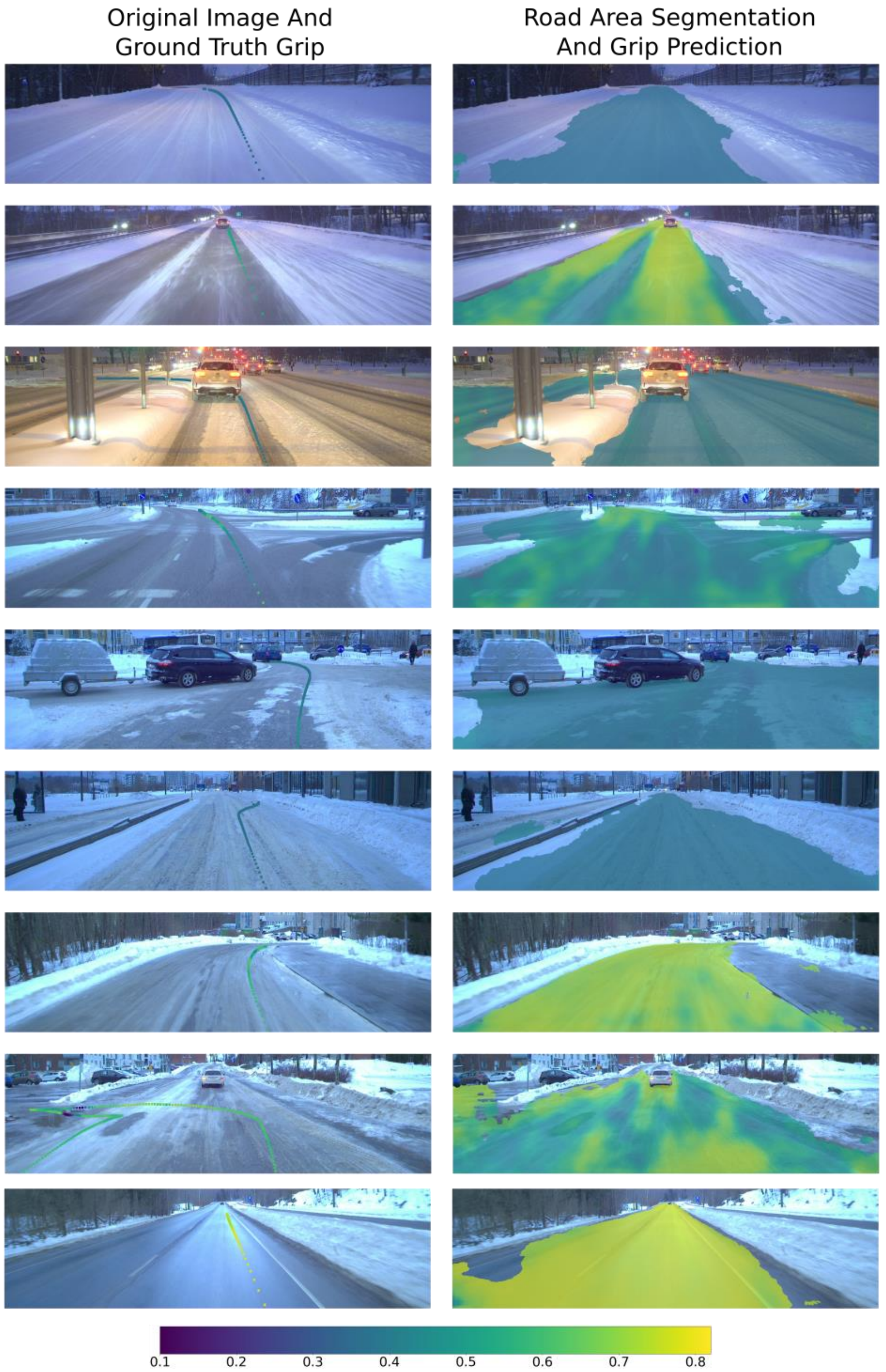

Figure 9. Examples of road area segmentation combined with grip prediction.

5 V2X message exchange

Vehicle-to-everything (V2X) communications are utilized to share detected environmental conditions among road participants. In deliverable ROADVIEW deliverable 5.3 [12] , we conducted a review of V2X messages that are relevant to the targeted environment conditions and use cases defined in [10], [11] for ROADVIEW. The conclusion drawn for sharing road weather information was to employ a Road Weather Message (RWM), adapted from SAE J2945-3 standard [5].

In this section, it will be initially outlined the software architecture of V2X communication units that are implemented for a Road Weather C-ITS service. Following this, the V2X message exchange and the structure of the Road Weather Message will be delved. Lastly, examples demonstrating the use of the V2X message exchange in relation to weather information sharing will be provided.

5.1 Communication units

The Vehicle-to-Everything (V2X) message exchange is implemented using cellular network connectivity and the MQTT (Message Queue Telemetry Transport) protocol. This approach manages the distribution of messages to various connected vehicles and the infrastructure-based systems, ensuring efficient and reliable communication. This setup facilitates seamless interaction between vehicles and the surrounding infrastructure, enhancing overall traffic management and safety.

As illustrated in Figure 10, the proposed V2X architecture supports the deployment of ROS nodes on the vehicle side, adhering to the ROS API defined in the ROADVIEW architecture D2.3 [7]. In contrast, the roadside unit does not utilize ROS nodes for exchanging V2X messages.

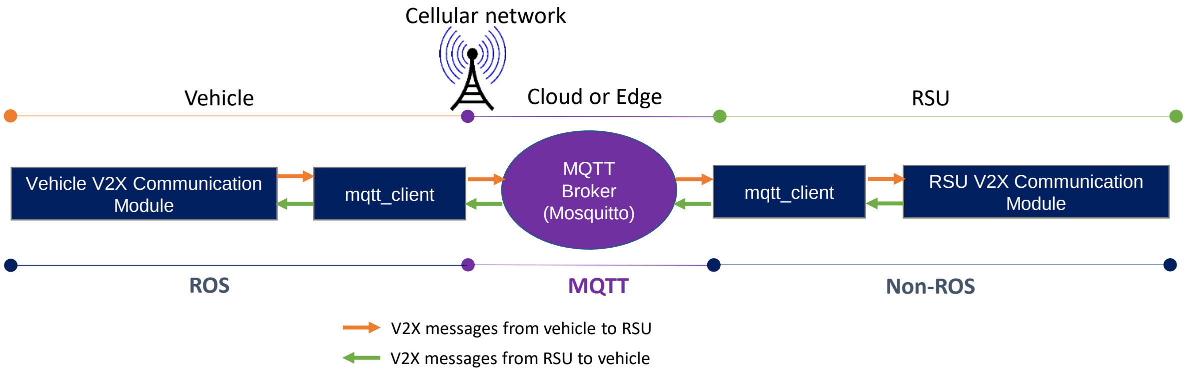

Figure 10. V2X Message exchanges through MQTT.

To facilitate communication between the MQTT topics and the ROS agent, the mqtt_client ROS package [4] is employed on the vehicle side. This package ensures seamless integration and message handling between the two systems. The MQTT broker is implemented using the Mosquitto open-source project [3]. Mosquitto provides a robust server supporting multiple versions of the MQTT protocol, including MQTT Version 5.0 (2019), ensuring compatibility and reliability in message transmission.

Figure 11 depicts the architecture of the V2X Communication Units specifically related to weather estimations. This setup enhances the system's ability to gather, process, and disseminate weather data, thereby improving the overall safety and efficiency of the V2X network. By integrating weather estimation capabilities, the architecture supports advanced features such as real-time weather alerts and adaptive driving strategies based on current and forecasted weather conditions. Overall, this V2X architecture demonstrates a sophisticated approach to vehicle and infrastructure communication, leveraging advanced technologies to promote a safer and more efficient transportation system.

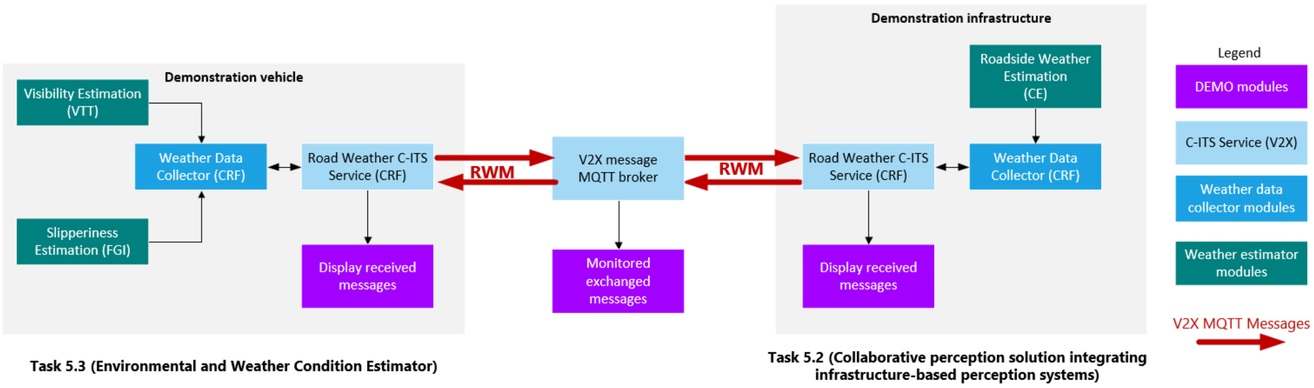

Figure 11. Architecture related to weather estimation and collaborative perception solution.

The left part of the figure illustrates the software modules within the demonstration vehicles. The visibility and slipperiness estimations, previously described in this document, are provided to a weather data collector module using a ROS API. This module stores the latest measurements for visibility and slipperiness, along with the corresponding times of measurement. The Road Weather C-ITS Service is responsible for generating and receiving Road Weather Messages (RWMs) using the MQTT protocol. The details of message exchange and structure will be further elaborated in section 5.2.

The right part of the figure pertains to the infrastructure-based perception system, which is detailed in [12]. This infrastructure system will receive RWMs and utilize them as described in section 5.3.2.

5.2 Message exchange

V2X messages are generated at a frequency of 1 Hz whenever the onboard weather estimators (visibility or slipperiness) have recent weather data to share, as illustrated in Figure 12.

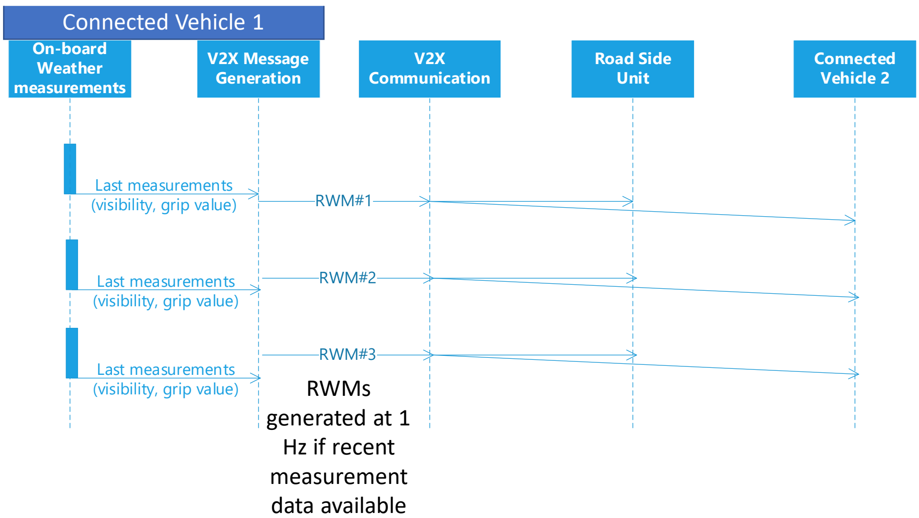

Figure 12. Road Weather Message sequence diagram.

The RWM generation event is scheduled to occur every second. If recent measurements of weather conditions are available, these results are included in the next RWM. If no measurements are available, the RWM generation is cancelled. Figure 13 shows the general structure of an RWM and highlights the sections of the message that are relevant to the onboard weather estimations described in this document.

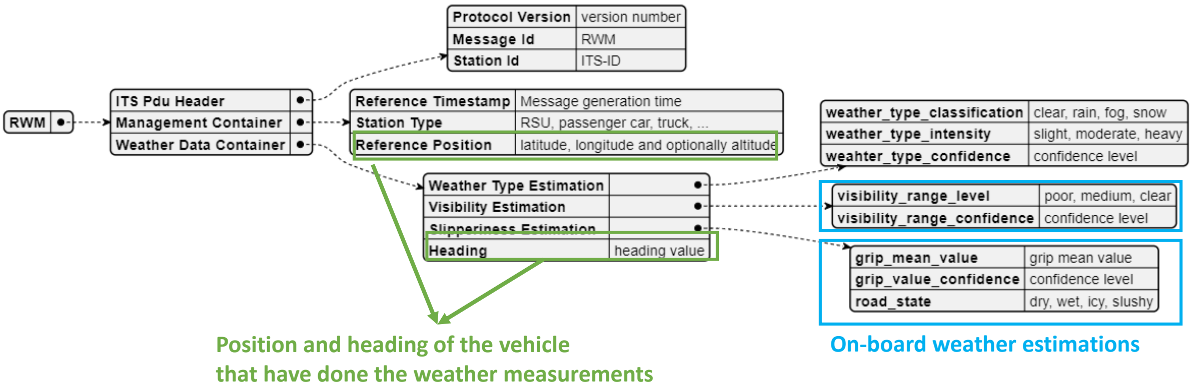

Figure 13. Road Weather Message Structure.

The ITS PDU Header, common to all V2X messages, contains the following:

- **Protocol Version and Message Type Identifier**: These allow the receiving ITS communication unit to verify if they can decode the message. The protocol version is set to "1," and the RWM message ID is "22".
- **ITS Station ID**: This identifies the sending ITS communication unit.

The Management Container part includes:

- **Reference Time:** The time when the message was generated.
- **Position:** The position of the sending ITS communication unit at the reference time.
- **Type of ITS Station:** This indicates the type of ITS station sending the message. The value is "5" for passenger cars and "7" for trucks. For roadside units, such as those performing weather classification estimations the value is "15".

The Weather Estimation Container includes the estimations obtained from various ROADVIEW weather estimation modules.

- **Visibility Estimation:** Aggregate the data from the visibility estimation module developed by VTT in Task 5.3. The data elements described in Table 2 may contain final adjustments in integration phase
- **Slipperiness estimation:** Provide data from the slipperiness estimation module developed by FGI in Task 5.3. The data elements described in Table 3 may also be updated when integrating the components

Table 2. Visibility estimation data elements.

Data element	Value
Visibility range level	Unavailable (0) Poor (1) Medium (2) High (3)
Visibility range level confidence	Confidence level value between 0 (no confidence) and 100 (full confidence) Unavailable (101)

Table 3. Slipperiness estimation data elements.

Data element	Value
Grip mean value	Value between 0 (no grip) and 100 (full grip) Unavailable (101)
Grip value confidence	Confidence level value between 0 (no confidence) and 100 (full confidence) Unavailable (101)
Road state	Unavailable (0), Dry (1), Wet (2), Icy (3), Slushy (4),

Here is an example of an RWM message in JSON format, generated by an onboard system with available measurements for visibility and grip values:


```
{"header": {"protocol_version": 1, "message_id": 22, "station_id": 5001}, "management_container": {"reference_time": 642967127198, "station_type": 5, "reference_position": {"latitude": 679558878, "longitude": 236806831, "altitude": 23920}}, "weather_data": {"visibility_range_level": 3, "visibility_range_confidence": 82, "grip_mean_value": 65, "grip_value_confidence": 68, "road_state": 2, "heading": 1487}}
```


In the next section, how the shared weather estimations can be utilized by other connected vehicles and infrastructure-based systems will be explored. Specifically, how these estimations enhance vehicle safety and enable proactive responses to adverse weather conditions will be examined. Tshe technical mechanisms involved in disseminating this data to ensure real-time updates and the seamless integration of weather information into various vehicular and infrastructural decision-making processes will be discussed.

5.3 Use of the V2X message with onboard weather estimations

5.3.1 Use by other connected vehicles

Connected vehicles receiving an RWM with visibility or grip values can be warned in advance about harsh weather conditions on the road. As shown in Figure 14, Vehicle 1 provides weather estimations indicating that a section of the road is icy. Vehicle 2, driving behind Vehicle 1, can receive this information before it detects the icy conditions itself. Additionally, Vehicle 3, which is driving on a non-icy road and will turn at the intersection, can also be warned about the icy road ahead and adjust its speed accordingly when turning right.

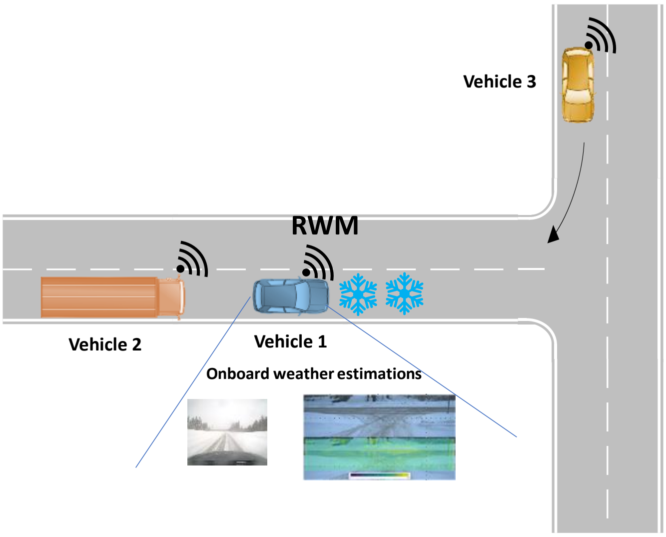

Figure 14. Use of RWM by other nearby connected vehicles.

One drawback is that only vehicles present at the same time as Vehicle 1 will receive the information. Vehicles arriving at this location later will not have access to this information.

5.3.2 Use by infrastructure-based system

When the roadside is equipped with an infrastructure-based V2I system, the RWMs can be collected by a roadside unit and used later to warn other vehicles approaching the monitored area about harsh road conditions, as illustrated in Figure 15.

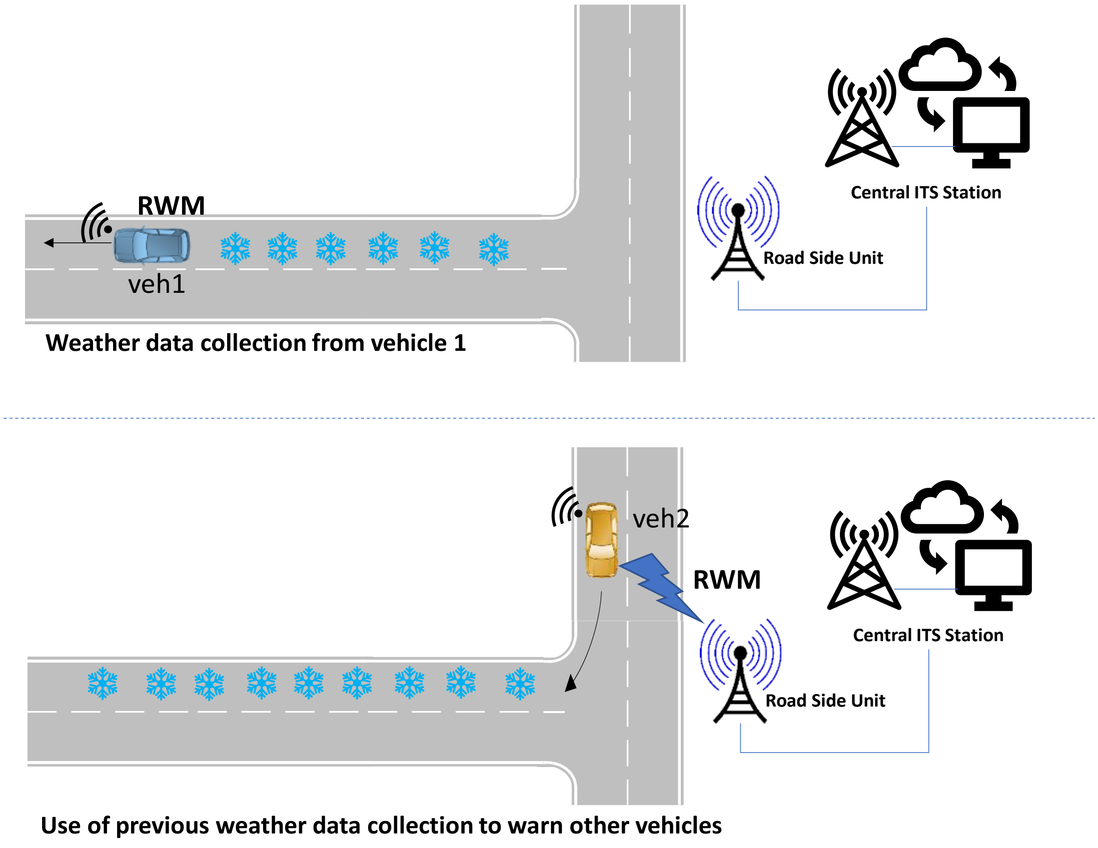

Figure 15. Reuse of previously collected RWM by other nearby connected vehicles.

The first vehicle, Vehicle 1, generated a series of RWMs while driving on the road near the roadside unit, indicating icy road conditions. The roadside unit monitoring the area collected this information, which remains relevant for a certain period of time. A second vehicle approaching this location can be warned by the roadside unit about the icy road conditions.

Additionally, the collected weather data will be used as input by the infrastructure-based decision-making system developed in WP6 to enhance overall road safety and traffic management.

Figure 16 displays a map of the monitored area, showing an example of weather data collected by the roadside unit. The left weather map shows the collected grip values, while the right weather map displays the visibility values, using a colour code to visually represent the received RWMs from vehicles driving in the monitored area. These collected weather values are considered valid for a certain period of time.

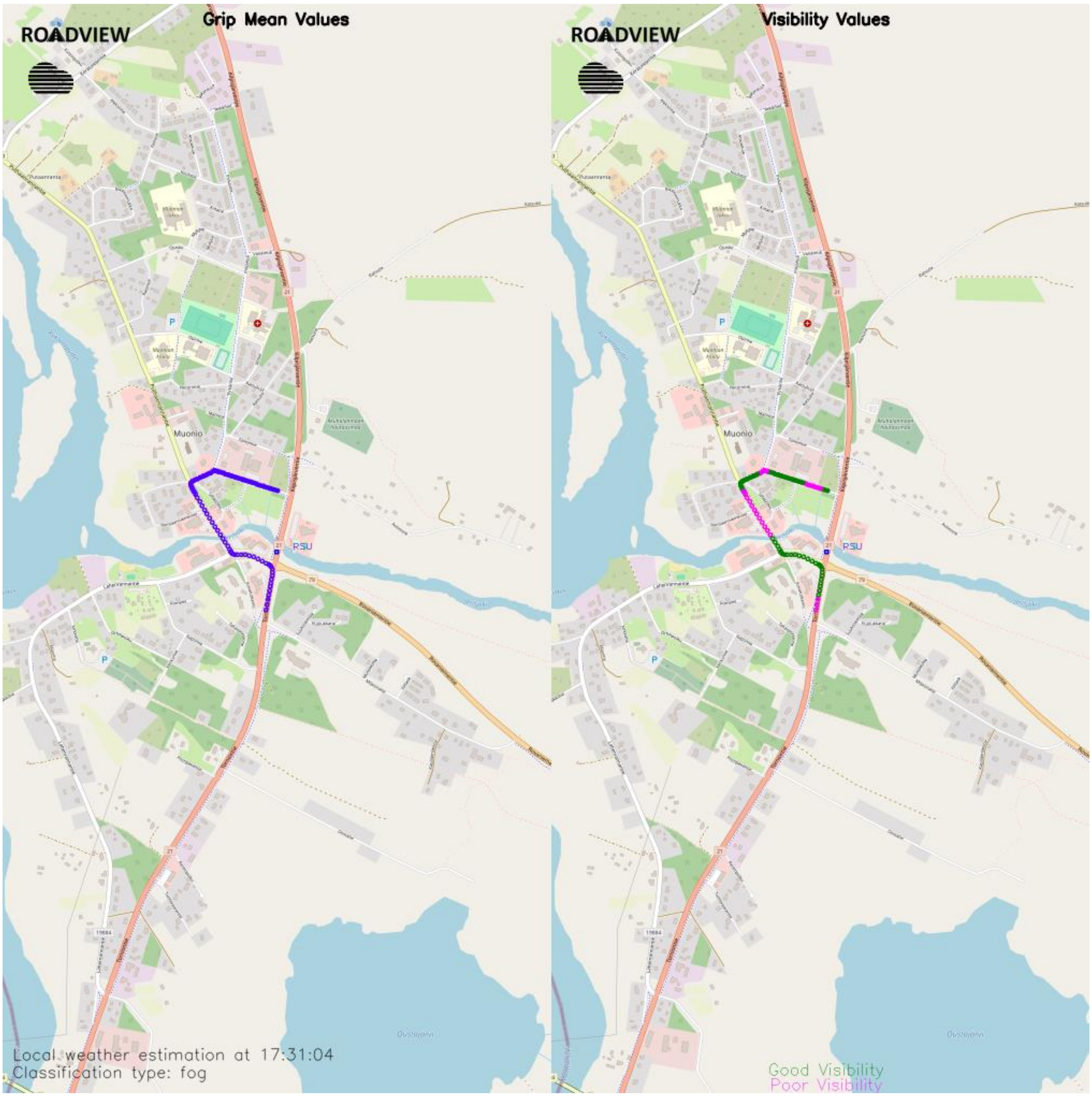

Figure 16. Weather data collection using collected RWMs by an infrastructure-based system.

6 Conclusions

This deliverable outlines the environmental condition monitoring work conducted to develop robust environmental perception modules for the ROADVIEW project. Three key functions create the framework for estimating the actual operational design domain (ODD) where the vehicle operates. These modules are:

- Visibility Estimator
- Slipperiness Monitoring
- Drivable Area Estimation

All modules utilize commercial optical sensing components, and the project has developed image processing algorithms that advance environmental awareness beyond the state-of-the-art in Level 3 automated vehicles.

Furthermore, this report covers the crucial aspect of the ROADVIEW project in utilizing existing infrastructure components. Although V2X technology has been under discussion in Europe since 2008, when the European Commission launched significant research projects in this domain, such as SAFESPOT under Framework Programme 6, the ROADVIEW solution is a turnkey approach [6]. It proposes a more collaborative sensing scheme, where more expensive infrastructure cameras support in-vehicle perception functions.

As a result, the project implements low-friction warnings in blind spots, such as intersections where parts of the road are obscured by buildings and bushes. This collaborative approach enhances safety and situational awareness, ensuring that vehicles receive timely warnings about potential hazards even in areas with limited visibility. Additionally, the project explores the integration of real-time weather data and road condition updates, further enhancing the accuracy and reliability of the system. By incorporating dynamic environmental data, the ROADVIEW solution can adapt to changing conditions, providing drivers and automated systems with the most current information to make informed decisions.

The collaborative sensing framework facilitates the creation of a connected vehicle network, where information is continuously shared between vehicles and infrastructure. This network can support various applications, such as traffic management, emergency response coordination, and efficient route planning. By enabling vehicles to communicate and cooperate, the system helps to optimize traffic flow, reduce congestion, and minimize the environmental impact of transportation.

The ROADVIEW project also emphasizes the importance of scalability and cost-effectiveness. By utilizing commercially available components and existing infrastructure, the project aims to provide a viable solution that can be easily implemented across different regions and vehicle types. This approach ensures that the benefits of the system can be widely accessible, promoting safer and more efficient transportation on a large scale.

7 References

[1] Narksri, P., Darweesh, H., Takeuchi, E., Ninomiya, Y. & Takeda, K. 2021 Visibility Estimation in Complex, Real-World Driving Environments Using High Definition Maps. IEEE International Intelligent Transportation Systems Conference (ITSC), Indianapolis, IN, USA, 2021, pp. 2847-2854
[2] Eclipse Mosquitto – An open source MQTT broker. available in [https://github.com/eclipse/mosquito]. cited on 2nd of July 2024.
[3] MQTT Version 5.0. available in [https://docs.oasis-open.org/mqtt/mqtt/v5.0/mqtt-v5.0.html]. cited on 2nd of July 2024.
[4] ROS mqtt client. available in [https://github.com/ika-rwth-aachen/mqtt_client]. cited on 2nd of July 2024.
[5] SAE International. Requirements for Road Weather Applications. SAE standard J2945-3. 2022. 87 p.
[6] SAFESPOT project. CORDIS EU results web site [https://cordis.europa.eu/project/id/026963]. Cited on 6th of June 2024.
[7] ROADVIEW. 2023. System reference architecture. Deliverable 2.3. ROADVIEW project ID: 101069576.
[8] Maanpää, J., Pesonen, J., Hyyti, H., Melekhov, I., Kannala, J., Manninen, P., Kukko, A. & Hyyppä, J. 2024. Dense Road Surface Grip Map Prediction from Multimodal Image Data. submitted to the International Conference on Pattern Recognition (ICPR). Kolkata, India. 1-5 Dec 2024.
[9] Maanpää, J., Melekhov, I., Taher, J., Manninen, P. & Hyyppä, J. 2022. Leveraging Road Area Semantic Segmentation with Auxiliary Steering Task. Image Analysis and Processing –21st International Conference - ICIAP 2022. Springer.. pp. 727-738.
[10] ROADVIEW. 2023. Definition of the complex environment conditions. Deliverable 2.1. ROADVIEW project ID: 101069576.
[11] ROADVIEW. 2023. Use Cases and Scenarios. Deliverable 2.2. ROADVIEW project ID: 101069576.
[12] ROADVIEW. 2023. SW on Collaborative Perception Solutions - First report. Deliverable 5.3. ROADVIEW project ID: 101069576.
[13] Acosta, M. Kanarachos, S., & Blundell, M. 2017. Road friction virtual sensing: A review of estimation techniques with emphasis on low excitation approaches. (MDPI, Ed.) Applied Sciences, 7, 1230.
[14] Kendall, A. & Gal, Y. 2017. What uncertainties do we need in bayesian deep learning for computer vision? Advances in neural information processing systems.
[15] Lin, T.-Y., Dollár, P., Girshick, R., He, K., Hariharan, B. & Belongie, S. 2017. Feature Pyramid Networks for Object Detection. Proceedings of the IEEE Conference on Computer Vision and Pattern Recognition (CVPR), 2117-2125.

[16] Ma, Y., Wang, M., Feng, Q., He, Z. & Tian, M. 2022. Current non-contact road surface condition detection schemes and technical challenges. Sensors, 9583.
[17] Neuhold, G., Ollmann, T., Bulò, S., R.. & Kontschieder, P. 2017. The Mapillary Vistas Dataset for Semantic Understanding of Street Scenes, 2017 IEEE International Conference on Computer Vision (ICCV), Venice, Italy, 2017, pp. 5000-5009.
[18] Ojala, R. & Seppänen, A. 2024. Lightweight Regression Model with Prediction Interval Estimation for Computer Vision-based Winter Road Surface Condition Monitoring. IEEE Transactions on Intelligent Vehicles, 1-13.
[19] Roychowdhury, S., Zhao, M., Wallin, A., Ohlsson, N. & Jonasson, M. 2018, Machine Learning Models for Road Surface and Friction Estimation using Front-Camera Images, 2018 International Joint Conference on Neural Networks (IJCNN), Rio de Janeiro, Brazil, 2018, pp. 1-8.
[20] Sakaridis, C., Dai, D. & Van Gool, L. 2021 ACDC: The Adverse Conditions Dataset with Correspondences for Semantic Driving Scene Understanding. 2021 IEEE/CVF International Conference on Computer Vision (ICCV), Montreal, QC, Canada, 2021, pp. 10745-10755.
[21] Open3D. Surface Reconstruction. available in [https://www.open3d.org/docs/latest/tutorial/Advanced/surface_reconstruction.html]. cited on 3rd of July 2024.